

Pure and almost pure NIR emission of Tm and Tm, Yb - CeO₂ under UV, X - ray and NIR up - conversion excitation: Key roles of level selective *antenna* sensitization and charge - compensation

Daniel Avram¹, Bogdan Cojocaru², Adriana Urda², Ion Tiseanu¹, Mihaela Florea² and Carmen Tiseanu¹

⁽¹⁾ National Institute for Laser, Plasma and Radiation Physics, P.O.Box MG-36, RO 76900, Bucharest-Magurele, Romania

⁽²⁾ University of Bucharest, Department of Chemical Technology and Catalysis, 4–12 Regina Elisabeta Bvd., Bucharest, Romania

(*) E-mail: tiseanuc@yahoo.com; carmen.tiseanu@inflpr.ro

Supplementary Information

Content:

Experimental details

Figure S1 XRD patterns, DR- UV/Vis – NIR and DRIFTs spectra of Tm - CeO₂ and Tm, Yb - CeO₂.

Figure S2. SEM images of Tm- CeO₂ and Tm, Yb – CeO₂.

Figure S3. Dependence of Tm - CeO₂ emission on gate width and time delay after the laser pulse.

Figure S4. Emission decays related to ¹G₄ and ³H₄ on excitation into Tm f – f absorption and CT band of CeO₂.

Figure S5. Broadening of Tm emission lines induced by Yb co – doping.

Figure S6. Dependence of Tm, Yb - CeO₂ emission on the delay time after the laser pulse under f-f excitation of Tm.

Figure S7. Variation of Tm, Yb - CeO₂ emission with excitation into Tm f – f absorption and CT band of CeO₂.

Figure S8. Dependence of Tm, Yb - CeO₂ UPC emission on the delay time after the laser pulse and dependence of NIR emission spectra on excitation into Tm f – f absorption.

Figure S9. UPC excitation spectra of Tm, Yb - CeO₂ measured around the emissions at 807, 653 and 494 nm.

Figure S10. Dependence of UPC emission intensity of Tm, Yb - CeO₂ (measured at 807 nm) on the pulse energy (excitation at 971 nm).

Experimental details

Materials: CeO₂ doped with Tm, Ho, Er (1%) or (co) doped with Yb (20 were synthesized by using the citrate complexation method. The calculated amount of Tm(NO₃)₃·6H₂O, Ho(NO₃)₃·6H₂O, Er(NO₃)₃·5H₂O, Yb(NO₃)₃·6H₂O and Ce(NO₃)₃·6H₂O were dissolved each in 25 ml hot distilled water (60°C). Then the corresponding solutions were mixed together and solid citric acid was added in order to obtain a ratio molar of metal ion: citric acid =1:1.2. The mixture was stirred on a hot plate at 60°C for 1h and then slowly evaporated in a vacuum rotavapor at 60°C until turned to a colourless gel. The gel was dried in an electrical oven at 60°C under vacuum for 5 h and at 120°C overnight, without vacuum. All samples were calcined at 1000°C with a heating rate of 10 °C/min for 5 hours.

Characterization: Powder X-ray diffraction (XRD) patterns were recorded on a Schimadzu XRD-7000 diffractometer using Cu K α radiation ($\lambda = 1.5418 \text{ \AA}$, 40 kV, 40 mA) at a scanning speed of 0.10 degrees min⁻¹ in the 5 – 90 degrees 2 Θ range. Diffuse reflectance optical (DR-UV-Vis) spectra were recorded at room temperature on a Analytik Jena Specord 250 spectrophotometer with an integrating sphere for reflectance measurements and MgO as the reflectance standard. DR-UV-Vis spectra of the materials were recorded in reflectance units and were transformed in Kubelka–Munk remission function F(R). Raman analysis was carried out with a Horiba JobinYvon - Labram HR UV-Visible-NIR Raman Microscope Spectrometer at 633, 514 and 488 nm. Fourier transform infrared (FTIR) spectra were measured with a Thermo Electron Nicolet 4700 FTIR spectrometer with a Smart Accessory for diffuse reflectance measurements. The IR spectra were scanned in the region of 4000–400 cm⁻¹ at the resolution of 4 cm⁻¹. The final spectra are an accumulation of 200 scans.

Optical and X-ray excited luminescence: The photoluminescence (PL) measurements were carried out using a Fluoromax 4 spectrofluorometer (Horiba) operated in both the fluorescence and the phosphorescence mode. The repetition rate of the xenon flash lamp was 25 Hz, the delay after flash varied between 0.03 and 4 ms and up to 30 flashes were accumulated per data point. Slits were varied from 5 to 29 nm for excitation and from 0.3 to 3 nm in emission measurements, respectively. The PL decays were measured by using the “decay by delay” feature of the phosphorescence mode. The average PL lifetime was calculated as integrated area of normalized decay. Time resolved emission spectra were recorded at 300K using a wavelength tunable NT340 Series EKSPLA OPO (Optical Parametric Oscillator) operated at 10 Hz as excitation light source. The tunable wavelength laser has a narrow linewidth < 4 cm⁻¹ with scanning step varying from 0.05 to 1 nm. As detection system, an intensified CCD (iCCD) camera (Andor Technology) coupled to a spectrograph (Shamrock 303i, Andor) was used. The time - resolved PL spectra were collected in the spectral range of 400 nm < λ_{em} < 900 nm by use of the box car technique using the time scale: $\delta t(\mu\text{s}) = 0.5 + 0.5 * (i)$, (where i= number of recorded spectra and δt is the delay after the laser pulse). Photoluminescence was detected with a spectral resolution of 0.88 nm and the input slit of the spectrograph was set to 10 μm . The temperature of the iCCD was lowered to -20 °C to improve its signal to noise ratio. For the energy dependence measurements, the spectra was measured with 500 accumulations to obtain a better signal to

noise ratio. The energy of the laser pulse was modified using neutral density filters and measured with a Gentec SOLO2 Laser Power & Energy Meter. PL spectra in the extended range of 400 to 1700 nm were measured by use of two Avantes spectrometers (AvaSpec-HS1024x58/122TEC for the range 400 ÷ 1100 nm and AvaSpec-NIR256-1.7TEC for the range 970 ÷ 1700 nm). Only the Avantes spectrometer AvaSpec-HS1024x58/122TEC was corrected by use of a calibrated Deuterium-Halogen light source (AvaLight-DH-S). Spectral resolution varied between 3.2 and 6 nm whilst the integration time varied between 100 to 5000 ms. For the acquisition of down-conversion emission spectra using AvaSpec-HS1024x58/122TEC, an 550 nm short pass filter was used to avoid CCD deterioration. X-ray induced emission was measured by use of X-ray tubes (Oxford Instruments, Apogee 5011, Mo target, focus spot ~40 µm, max. high voltage - 50 kV, max current - 1 mA). X-ray induced luminescence was collected in a coaxial transmission irradiation configuration with the sample holder placed at 40 mm of the X-ray focal spot. The emitted light was collected with a lens with focal distance of 8 mm on both Avantes spectrometers and the X-ray debit dose was up to 2 Gy/s. The characterization of the porous texture of the as-synthesized and calcined samples was performed by N₂ adsorption at -196°C using a Micrometrics instrument (ASAP 2010). The Brunauer-Emmett-Teller (BET) method was used to calculate the surface area from the data obtained at P/P₀ between 0.01 and 0.995. Prior to surface area determination, the samples were outgassed at 150°C for 5 h. The pore size distribution of each sample was determined from the desorption branch of the N₂ isotherm. Sample morphology was investigated by scanning electron microscopy (SEM) using a Jeol JSM-7001 F electron microscope.

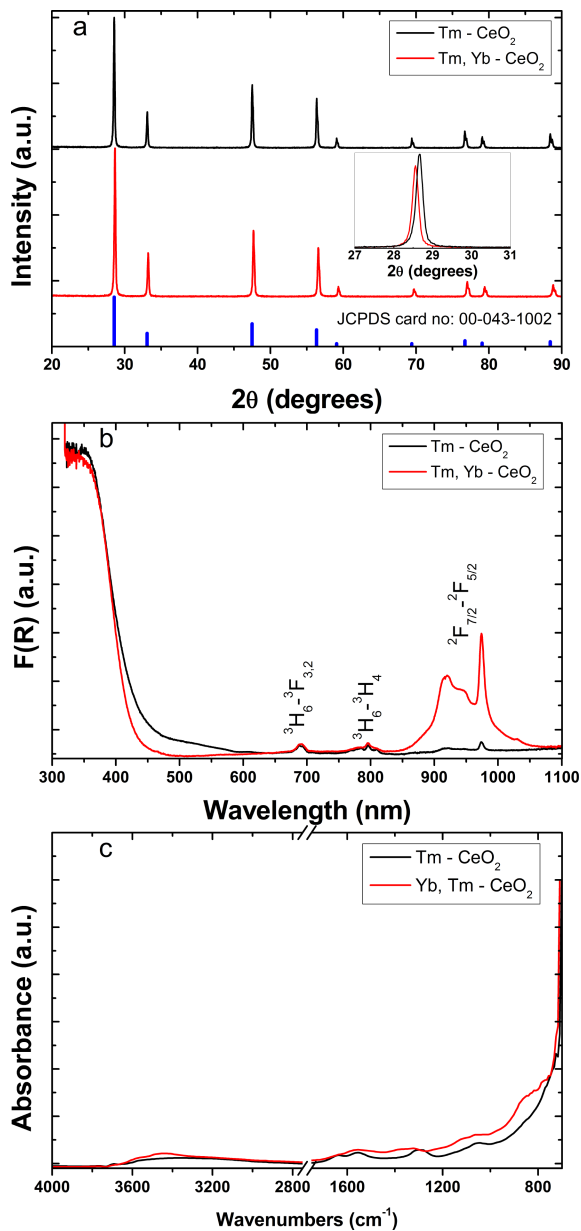


Figure S1 XRD patterns (a), DR-UV/Vis (b) and DRIFTS spectra (c) of Tm - CeO_2 and Yb, Tm - CeO_2 . In (a) XRD patterns for pure CeO_2 are also included.

DRIFTS spectra of Tm (1%) and Tm (1%), Yb (20%) doped CeO_2 samples Figure S1 (c) are quite similar and agree with spectra reported in literature^{S1-S3}. The bands in the frequency range from 1000 to 1700 cm^{-1} could be assigned to some traces of un-decomposed nitrates in the as-prepared sample and carbon based impurity species, as follows: the band at around 1300 cm^{-1} is most probably due to the presence of small amount remnant nitrates and the band at 1600 cm^{-1} is due to CO_2 from atmosphere. The less intense peak at 1100 cm^{-1} might be due residual organics which is present in both samples.

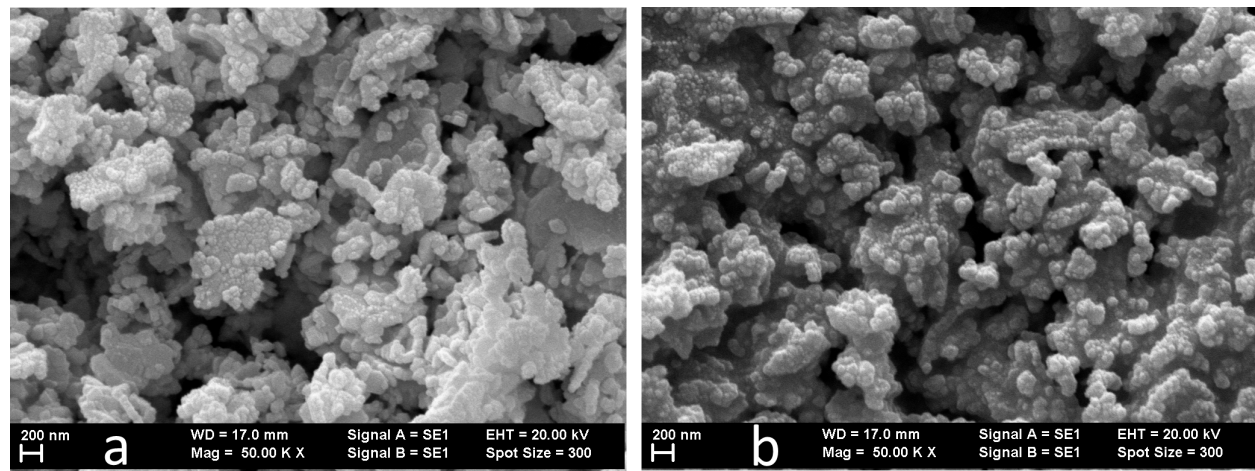


Figure S2. SEM images of Tm- CeO₂ (a) and Tm, Yb – CeO₂ (b) that show conglomerates of small crystallites with sizes around 40 - 50 nm in agreement with crystallite size estimated from XRD patterns.

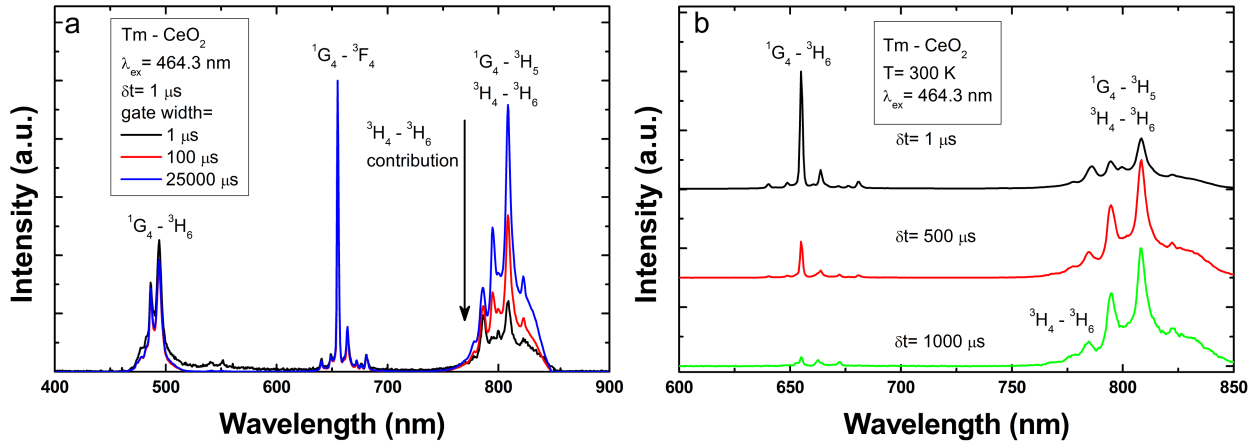


Figure S3. Dependence of Tm - CeO₂ emission spectra on gate width (a, spectra were normalized at 494 nm) and time delay (b) after the laser pulse. The spectra show that the emission around 800 nm is a mixture between the longer-lived $^3\text{H}_4$ emission and shorter lived $^1\text{G}_4$ emission.

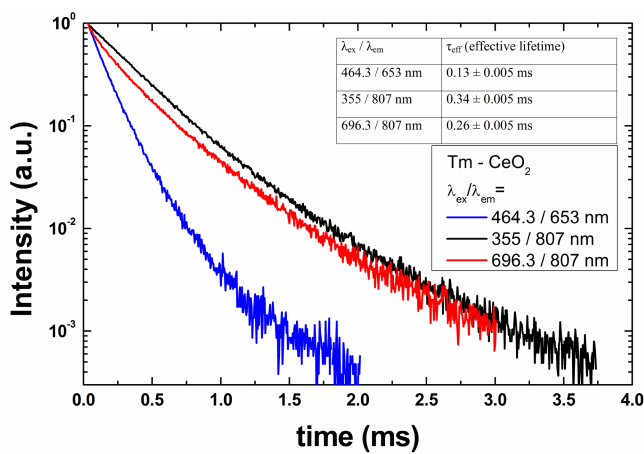


Figure S4. Emission decays of Tm – CeO₂ corresponding to ¹G₄ and ³H₄ levels under down-conversion excitation. A slightly longer lived emission was measured for ¹H₄ level when excited into the charge-transfer (CT) of CeO₂ compared to f-f excitation.

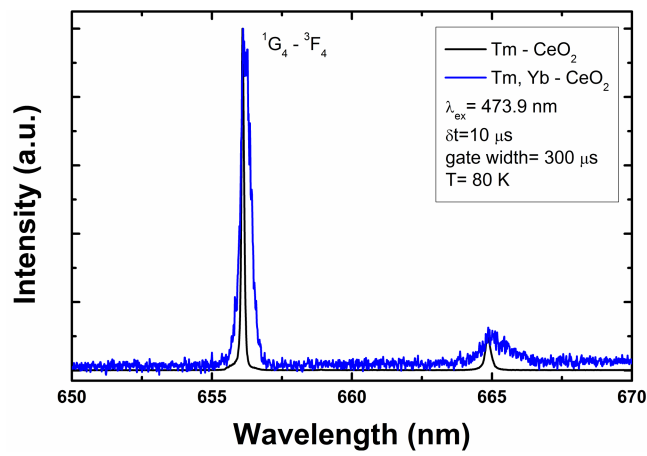


Figure S5. Broadening of Tm emission induced by Yb co – doping in Tm, Yb – CeO₂.

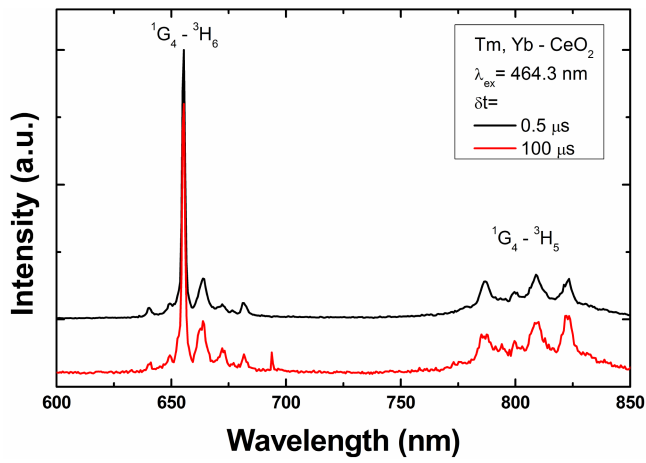


Figure S6. Dependence of Tm, Yb - CeO₂ emission spectra on the delay time after the laser pulse under f-f excitation of Tm showing only the contribution from $^1\text{G}_4$ level.

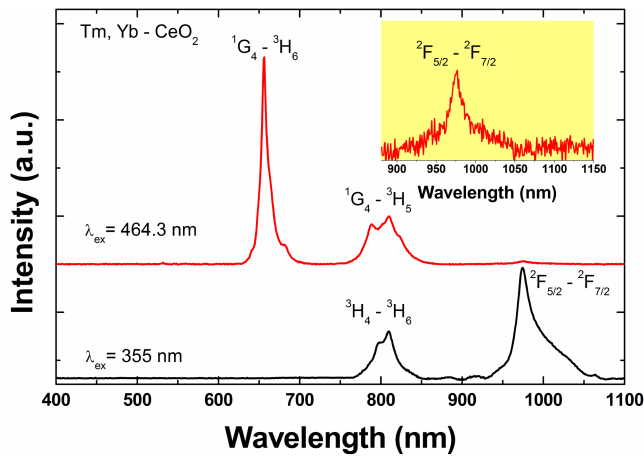


Figure S7. Comparison between Tm, Yb - CeO₂ emission spectra under f-f and CeO₂ CT excitation. Both spectra have weak intensity. The presence of Yb emission in the CT excited spectrum may be due to sensitization of Yb emission *via* ceria CT band as previously reported.^{S4}

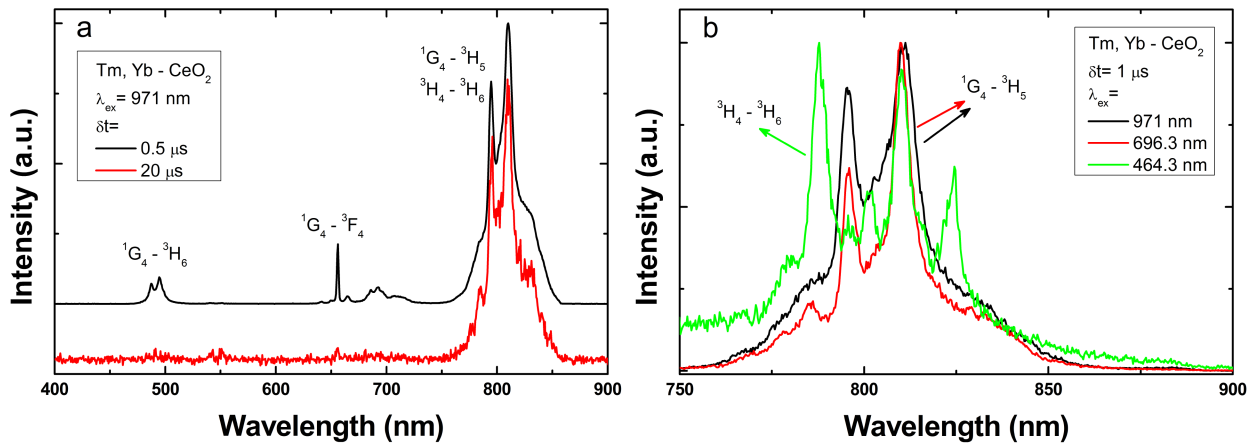


Figure S8. Dependence of Tm, Yb - CeO₂ UPC emission spectra on the delay time after the laser pulse (a) and dependence of NIR emission of Tm around 800 nm on the excitation wavelength (b).

Figure S8a highlights the merit of time-gated UPC ⁵⁵ in differentiation of the strongly overlapped $^1\text{G}_4$ and $^3\text{H}_4$ emission around 800 nm.

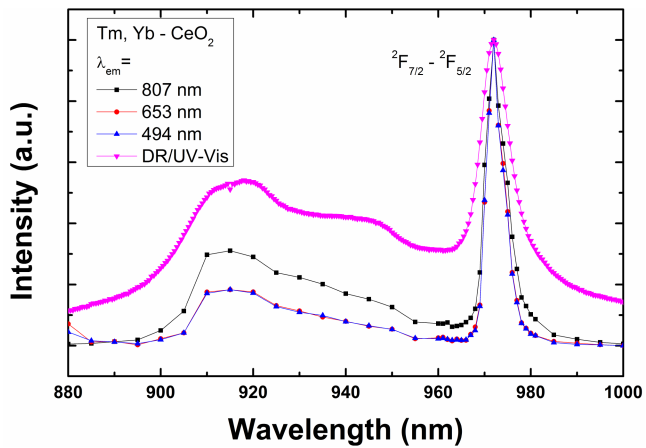


Figure S9. UPC excitation spectra of Tm, Yb - CeO₂ that monitor the Tm emission at 807, 653 and 494 nm. For comparison, the DR/UV-Vis – NIR spectrum is also included.

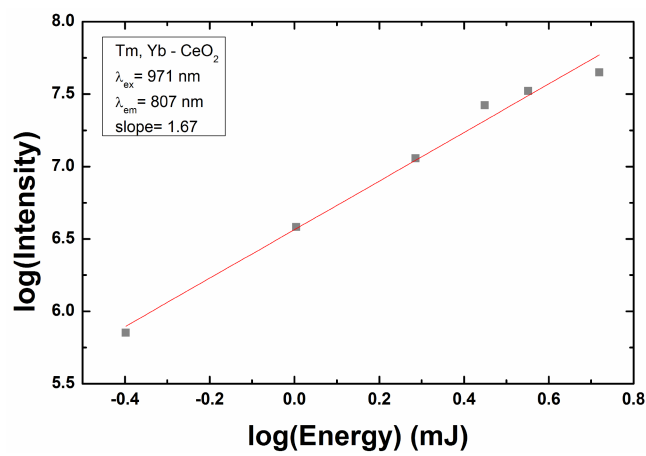


Figure S10. Dependence of Tm, Yb - CeO₂ UPC emission intensity at 807 nm on the pulse energy at 971 nm. The dependence confirms a two-photon mechanism.

References:

- S1. M. L. Dos Santos, R. C. Lima, C. S. Riccardi, R. L. Tranquillin, P. R. Bueno, J. A. Varela and E. Longo, *Materials Letters*, 2008, **62**, 4509.
- S2. K.C. Anjaneya, G.P. Nayaka, J. Manjanna, G. Govindaraj and K.N. Ganesh, *J. Alloys Comp.*, 2014, **585**, 594.
- S3. H. P. Dasari, J. S. Ahn, K. Ahn, S.-Y. Park, J. Hong, H. Kim, K. J. Yoon, J.-W. Son, H.-W. Lee and J.-H. Lee, *Solid State Ionics*, 2014, **263**, 103.
- S4. Ueda and S. Tanabe *J. Appl. Phys.*, 2011, **110**, 073104.
- S5. C. Tiseanu, V. Parvulescu, D. Avram, B. Cojocaru, N. Apostol, A. V. Vela-Gonzalez and M. Sanchez-Dominguez, *Phys. Chem. Chem. Phys.*, 2014, **16**, 5793.